Analysis of the Atomic Layer Deposited Al_2O_3 field-effect passivation in black silicon

Guillaume von Gastrow[a*], Ramon Alcubilla[b], Pablo Ortega[b], Marko Yli-Koski[a], Sònia Conesa-Boj[c], Anna Fontcuberta i Morral[c], and Hele Savin[a]

[a]Aalto University, Department of Micro- and Nanosciences, Tietotie 3, 02150 Espoo, Finland

[b]Universitat Politècnica de Catalunya, Dept. Enginyeria Electrònica, C/ Jordi Girona 1-3, Modul C4, E - 08034 Barcelona, Spain

[c]Laboratory of Semiconductor Materials, Ecole Polytechnique Fédérale de Lausanne (EPFL), 1015 Lausanne, Switzlerland

*Corresponding author: Tel.: +358504316367; e-mail address: guillaume.von.gastrow@aalto.fi

We demonstrate that n-type black silicon can be passivated efficiently using atomic layer deposited (ALD) Al_2O_3, reaching maximum surface recombination velocities below 7 cm/s. We show that the low surface recombination velocity results from a higher sensitivity of the nanostructures to surface charge and from the absence of surface damage after black silicon etching. The surface recombination velocity is shown to be inversely proportional to the fourth power of the negative charge in contrast to the quadratic dependence observed in planar surfaces. This effect compensates the impact of the increased surface area in the nanostructures and extends the potential of black silicon for instance to n-type Interdigitated Back Contact (IBC) cells.

Keywords: Nano-texturing; Surface passivation; Reactive Ion Etching; Negative charge; Al_2O_3; Atomic Layer Deposition

1. INTRODUCTION

Black silicon, i.e. nanostructured silicon surface, reduces sun light reflectance significantly as compared to conventional random pyramids [1], and thus is an extremely promising material for photovoltaic applications. However, the first attempts to integrate black silicon into solar cells [2-4] showed only modest conversion efficiency values due to severe surface recombination. The increased recombination activity was explained

mainly by the large black silicon surface area [3] and by possible etching damage [5]. The recombination issue in p-type black silicon has recently been overcome using reactive ion etching to form the black silicon and Atomic Layer Deposited (ALD) Al_2O_3 to passivate the surfaces, with maximum surface recombination velocities ranging between 13 cm/s and 80 cm/s [6-8]. The excellent surface passivation is demonstrated by internal quantum efficiency values close to 100 % in black silicon solar cells [9].

It is known that the high-quality surface passivation obtained with ALD Al_2O_3 on planar silicon [10,11] is due to the high fixed negative charge and to the low defect density at the interface between silicon and Al_2O_3 [12,13]. However, the properties of the Si/Al_2O_3 interface cannot explain alone the similar passivation levels obtained in planar and ~~in~~ nanostructured silicon due to much larger surface area present in the latter. Consequently, it has been speculated that the efficient black silicon passivation by Al_2O_3 could arise from the strong field-effect generated by the fixed Al_2O_3 charge that leads to repulsion of charge carriers from the entire black silicon needles [6,14]. However, no clear evidence has been given so far. Hence, we study here systematically the impact of the fixed charge density on the passivation performance of black silicon and we propose a more detailed explanation for the very low recombination velocities experimentally achieved.

2. EXPERIMENTAL DETAILS

The experiments were performed on double-side polished Magnetic Czochralski phosphorus-doped wafers (100) oriented and of resistivity (3.3 ± 0.5) Ω·cm, corresponding to a doping concentration of $(1.4 \pm 0.2)\cdot 10^{15}$ cm^{-3}. The wafer thickness was 445 µm and the oxygen level was 8.0 ± 0.1 ppma.

Black silicon was formed on both sides of the wafers by reactive ion etching (RIE) in an Oxford Instruments Plasmalab System100 - ICP 180 tool. The samples were etched in SF_6/O_2 plasma for 7 min at a temperature of -120 °C and at a pressure of 10 mTorr. The SF_6 and O_2 flow rates were set to 40 and 18 sccm, and the powers of inductively and capacitively coupled power sources were 1000 W and 2 W, respectively.

The black silicon and the planar reference samples (without black silicon) were then passivated by 20 nm of ALD Al_2O_3 using a Beneq TFS 500 tool after a 1 % HF dip for 60 s. The oxide was deposited on both sides of the samples using TMA (Sigma-Aldrich, 97

% purity) and water as precursors. Then, the film thickness was measured by a Plasmos SD2300 Ellipsometer at a wavelength of 632.8 nm. The film depositions were followed by an anneal at 425 °C for 30 min in N_2. The charge at the Si/Al_2O_3 interface as well as surface potential maps were measured after annealing using the COCOS (Corona Oxide Characterization of Semiconductors) technique [15,16].

The dependence of surface recombination velocity on effective surface charge was studied by measuring the minority carrier lifetime after adding successive Corona charge steps. Surface potential maps were measured after this study in order to calculate the total charge deposited. Both oxide charge and potential maps were measured using the Semilab SDI PV2000 tool. The lifetimes were measured by Quasi-Steady State Photoconductance (QSSPC) with a Sinton WCT-120 tool and the values were taken at an injection level of $1\cdot10^{15}$ cm^{-3}.

The effective surface recombination velocity (S_{eff}) was extracted from the QSSPC measurements using the following expression:

$$S_{eff} = \frac{W}{2}\left(\frac{1}{\tau_{eff}} - \frac{1}{\tau_{bulk}}\right) \qquad (1)$$

where W is the wafer thickness, and τ_{eff} and τ_{bulk} represent the measured effective and bulk lifetimes, respectively. When assuming an infinite bulk lifetime, as in section 3.1, Eq. 1 results in the maximum effective surface recombination velocity. In section 3.3, however, the bulk lifetime was taken into account to obtain reliable slopes values. The bulk lifetime was estimated at 6 ms, which corresponds to the highest lifetime measured in the same planar substrate passivated by Al_2O_3.

A soft mechanical contact between the black silicon sample and a holey carbon grid resulted in the transfer of the nanoscale silicon needles to the grid for observation in the transmission electron microscope. The structure and composition of the material was studied by transmission electron microscopy and electron dispersive X-ray spectroscopy in a FEI Tecnai OSIRIS microscope operated at 200 kV using the Super-X (0.9 radian collection angle) detector and the Bruker Esprit software.

3. RESULTS

3.1. Surface morphology and passivation quality

A high resolution Scanning Electron Microscopy (SEM) picture of the black silicon used in this study is presented in Figure 1a. A platinum layer was sputtered on top of the black silicon in order to enhance the contrast of the Al_2O_3 film, which appears lighter on the picture. A highly conformal ALD Al_2O_3 layer can be observed on the entire surface of the black silicon needles. Note that the importance of the deposition technique can be seen from the voids in the platinum layer, as the conformality of sputtered film is not sufficient to fully coat the needles. The reflectance of bare black silicon is displayed in Figure 1b and shows that a reflectance below 1 % is achieved in the whole visible spectrum as well as in the near UV and near IR regions. As a comparison, the reflectance of random pyramids without antireflection coating varies between 10 % and 30 % in the same wavelength range.

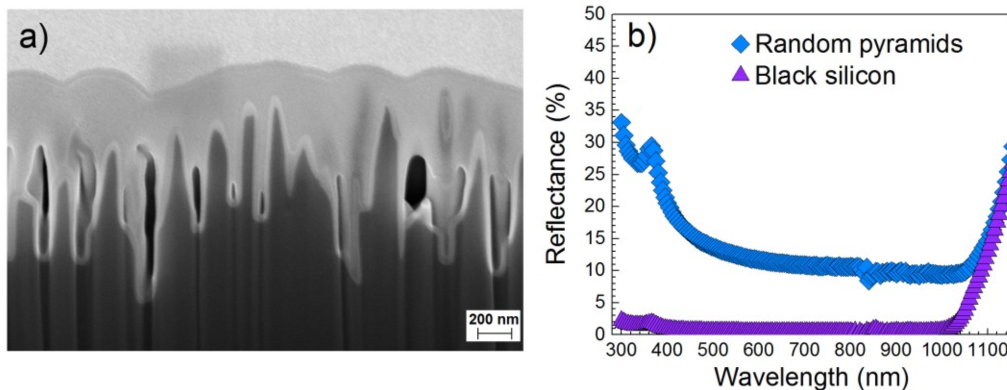

Figure 1: a) SEM picture of a black silicon section b) Reflectance curves of a black silicon sample and of a sample with random pyramid structures, both without antireflection coatings.

Figure 2 shows the minority carrier lifetime as a function of injection level measured both in black silicon and planar silicon wafers. Despite the high surface area of black silicon and the potential surface damage induced by the etching process, a minority carrier lifetime of more than 3 ms was obtained in black silicon, corresponding to a maximum surface recombination velocity (SRV) of less than 7 cm/s. The passivation quality is almost as high in black silicon as in planar substrates, where maximum surface recombination velocities of 4 cm/s were measured.

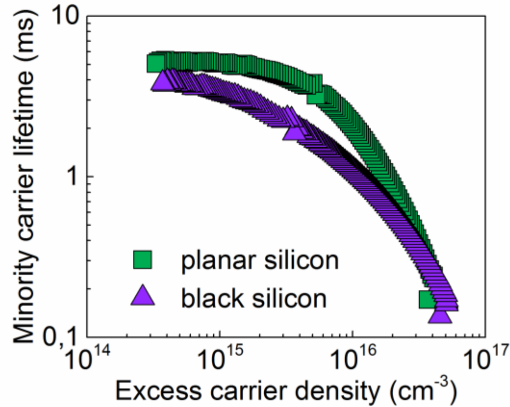

Figure 2: Comparison of the minority carrier lifetime obtained in black silicon and planar samples coated with 20 nm of Al_2O_3 and annealed at 425 °C for 30 min.

As in planar silicon, both the interface defect density and the total dielectric charge density are relevant parameters to characterize the surface passivation quality of silicon nanostructures. In addition, some damage is likely to happen during the RIE process [5], and a loss of crystallinity is usually observed within the 20 first nanometers of the nanostructures [17].

The potential damage occurring in silicon after black silicon etching was studied with the help of high resolution Transmission Electron Microscopy (TEM) measurements, as shown in Figure 3. In Figure 3a, we illustrate a low magnification bright field TEM image, where a complete black silicon needle can be observed in dark grey, while the Al_2O_3 is depicted by a lighter grey layer that covers the base and the tip of the needle with a thickness variation of less than one nanometer. Such chemical configuration has been confirmed by energy-dispersive X-ray spectroscopy (EDX), as shown in Figure 3b. Electron diffraction was performed within the 20 first nanometers of a black silicon needle (see Figure 3c), and the fast Fourier Transform in the inset of Figure 3c shows that the crystallographic structure of silicon was preserved, thus proving that the etching process is not substantially harmful to the silicon surface. As a result, a good chemical passivation can be obtained, which explains the high lifetimes observed.

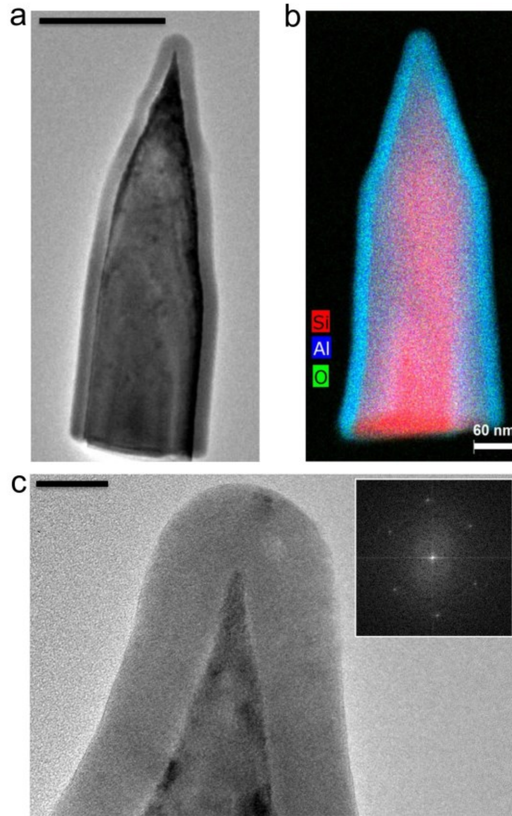

Figure 3: (a) Low magnification bright field TEM image of one representative black silicon needle. The scale bar in (a) is 200 nm; (b) Chemical compositional map performed by EDX, where the red, blue and green colors correspond respectively to Si, Al and O signals; and (c) high resolution TEM image performed in the tip of the needle and corresponding fast Fourier transform (inset of c). The scale bar in (c) is 20 nm.

3.2. Modeling the effect of the surface charge on surface potential and depletion width

Even though the surface crystallinity of our samples is not affected by the etching process, the chemical passivation achieved in nanostructures cannot explain alone the similar surface recombination values in planar silicon and in black silicon due to the increased surface area of the nanostructures. Thus, an enhanced field-effect passivation is likely to be responsible for the high black silicon lifetimes [6]. In n-type substrates, a negative surface charge will repel majority carriers from the surface, leading to the so-called depletion regime. If the charge is high enough, inversion from n-type to p-type takes place near the surface. Strong inversion naturally results in lower recombination at

the surface, as the probability of a recombination event is smaller due to the low electron density.

Since the Al_2O_3 used in this study is well known to provide a relatively high negative charge density, the entire nanostructures are expected to be depleted. To confirm this hypothesis, a threshold charge density for strong inversion in n-type planar silicon was calculated by solving Poisson's equation in one dimension [18]. Figure 4a shows that a strong inversion can be reached easily with Al_2O_3 for a wide range of resistivities. Although 1D models may not be directly applicable to black silicon, Figure 4b suggests that the nanostructures are indeed fully depleted.

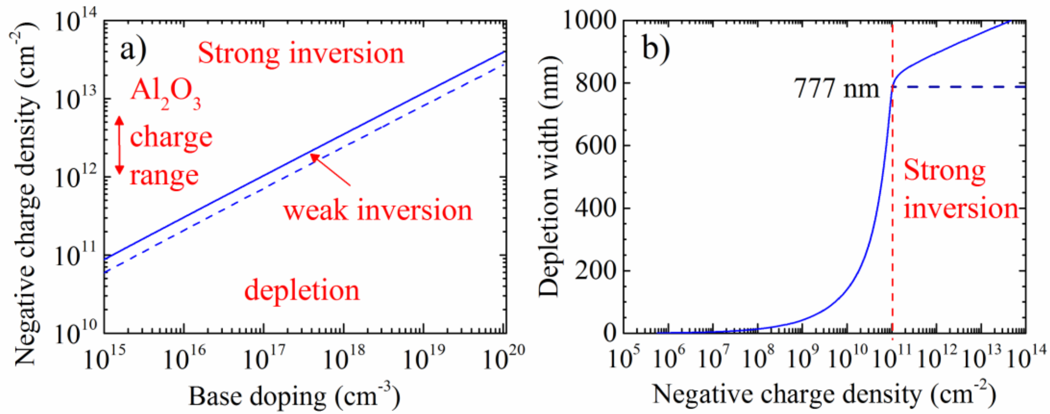

Figure 4: a) Threshold surface charge for weak inversion (dashed line) and strong inversion (plain line) on planar n-type silicon for different base doping values. The typical charge densities measured in Al_2O_3 are also shown. b) Evolution of the depletion region width with the charge density in planar n-type silicon of doping $1.3 \cdot 10^{15}$ cm^{-3}. In strong inversion, the depletion width no longer depends on the charge density, as depicted by the blue dashed line.

3.3. Effect of surface charge on surface recombination velocity in black silicon

The results shown in Figure 4 do not provide information about a possible enhancement of the field effect due to the black silicon geometry. Due to the shape of the needles, the Al_2O_3 fixed charges from the entire cone surface contribute to the total electric field inside a black silicon needle, providing an enhanced electric field. The surface area ratio between black silicon and a planar surface was estimated from SEM pictures and was found to be 7 – the shape of a needle can typically be approximated by a cone of 700 nm height and 200 nm base diameter (see the inset of Figure 5a). Thus, a similar charge

should be found in planar silicon and in black silicon by multiplying the measured planar silicon charge by a factor of 7.

The measured fixed charge at the interface between Al_2O_3 and silicon are shown in Figure 5a. The charge density is much higher in black silicon ($9.9\cdot10^{12}$ cm^{-2}) than in the corresponding planar sample ($2,4\cdot10^{12}$ cm^{-2}). However, after re-scaling by a factor of 7, the charge densities are found similar in both samples. Consequently, the charge measured in black silicon can be considered as an effective charge density, and the high measured value compared to the planar reference is explained by the larger surface area. This result also implies that COCOS measurements seem to be applicable to black silicon structures as well.

Positive corona charge was then applied on both sides of black silicon sample to study the effect of surface charge on the passivation, together with a reference planar sample with the same thickness of aluminium oxide. The effective surface recombination velocities (SRV) were extracted from the effective lifetime measurements assuming a finite bulk lifetime, as explained in the section 2. The SRV was then plotted as a function of the total effective negative charge present on the sample surface. The slopes of the inversion part of the curves were measured in several samples and Figure 5b presents the typical curves obtained.

The surface recombination velocity of p-type planar samples in inversion has been shown to be inversely proportional to the square of the charge density present on the surface of a planar sample [19,20]. This can be extended to n-type samples as well:

$$S_{eff} = 2\varepsilon_S \frac{kT}{q^2} \frac{N_D S_{n0}}{(Q_f)^2} \quad (2)$$

where S_{eff} is the effective surface recombination velocity (m/s), S_{n0} is the fundamental recombination velocity of electrons (m/s), N_D is the base doping (m^{-3}), ε_S is the product of the vacuum permittivity and of the dielectric constant of silicon (F·m^{-1}), q is the fundamental charge (C), k is Boltzmann's constant (J·K^{-1}), T is the temperature (K) and Q_f is the total surface charge (m^{-2}).

This dependence is in agreement with our result in the reference samples, where a slope of -2.0 ± 0.5 was found. However, the dependence is much stronger in the case

of black silicon samples, where a slope of -3.9 ± 0.6 was measured. This means that the charge has a decisive effect on the passivation of black silicon structures, which can be explained by the geometry of the nanostructures. At low charge density, the edge of the depletion region follows the shape of the nanostructure, while at high charge densities, the region flattens and penetrates deeper in the silicon bulk. At higher charge densities, the effective recombination-active surface area seen at the macroscopic scale in black silicon becomes smaller and approaches that of planar silicon, which results in improved passivation.

Note that some charge leakage probably occurred in the Al_2O_3 layers, as the surface potential measurements revealed that the final Corona charge deposited did not reach the expected charge of $+5\cdot10^{12}$ cm^{-2}. Based on the leakage observed in our samples and previous studies [21], an error of 15 % was estimated in the charge measurements.

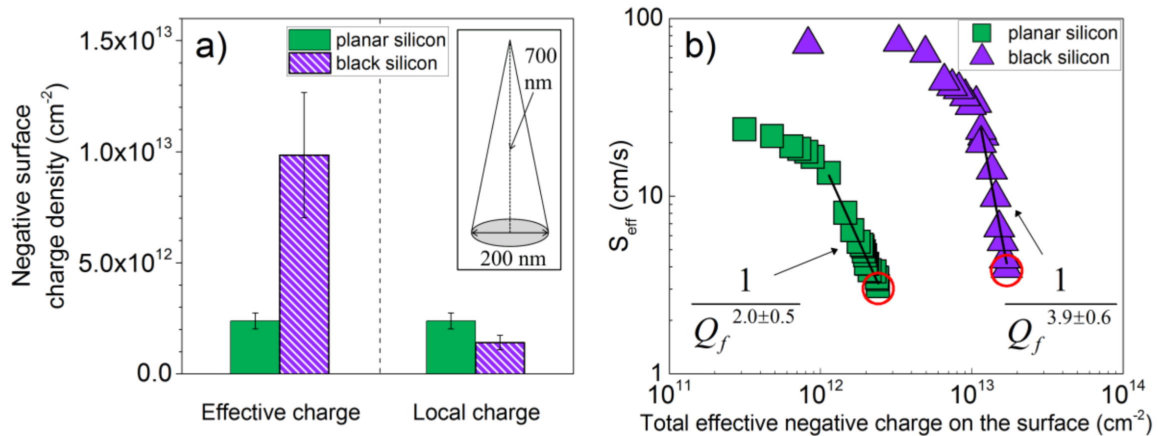

Figure 5: a) Average Al_2O_3 charge density measured on planar and black silicon samples passivated with 20 nm of Al_2O_3. An effective charge density is seen at the macroscopic scale. The local charge density was obtained by taking into account the surface area enlargement in black silicon. The inset presents a schematic of a typical b-Si needle. b) Maximum surface recombination velocity as a function of the total negative charge after corona charging on both sides of the samples. The total charge corresponds to the sum of the corona charge and of the built-in Al_2O_3 charge, and the circles show the initial measurement points before Corona charging.

Although all the experiments in this study were performed on n-type silicon, it is likely that the conclusions are applicable to p-type silicon as well. Simulations have predicted a

similar dependence on surface charge in accumulated p-type silicon and in inverted n-type silicon [19]. Therefore, an enhanced field-effect due to the geometry could also explain the high lifetimes obtained in p-type black silicon passivated by ALD Al_2O_3 [6,8].

4. CONCLUSIONS

We have studied the passivation of n-type black silicon using ALD Al_2O_3. Unlike reports from other studies, we did not observe critical crystal damage of the nanostructured surface after the RIE process. The negative charge present in Al_2O_3 creates a strong inversion and results in excellent passivation in a wide range of doping densities. Black silicon was shown to be more sensitive to the surface charge than planar surfaces due to geometrical effects. As a result, surface recombination velocities were shown to be inversely proportional to the fourth power of the surface charge in inverted n-type black silicon. The minority carrier density is consequently highly reduced near the nanostructured surface, resulting in excellent passivation without a need for tradeoffs in reflectance.

To conclude, those results imply that there is potential for raising black silicon passivation to the level of planar silicon, for instance with the help of higher fixed charge dielectrics.

ACKNOWLEDGMENTS

This work was funded by the Energy Efficiency Research Program of Aalto University School of Electrical Engineering (Effinano project number 91581015). The ERC starting grant UpCon No. 239743, the project NanoTera Synergy, as well as the project NOE Nanophotonics for Energy are also acknowledged. This research was undertaken at the Micronova Nanofabrication Centre, supported by Aalto University, as well as at BarcelonaTech and at the Interdisciplinary Centre for Electron Microscopy in Lausanne, Switzerland. The authors would also like to thank Dr. Trifon Trifonov for the SEM characterization.

Reference List

[1] P.B. Clapham, M.C. Hutley, Reduction of Lens Reflexion by the "Moth Eye" Principle, Nature. 244 (1973) 281-282.

[2] S. Jeong, M.D. McGehee, Y. Cui, All-back-contact ultra-thin silicon nanocone solar cells with 13.7% power conversion efficiency, Nat Commun. 4 (2013) 2950.

[3] J. Oh, H. Yuan, H.M. Branz, An 18.2%-efficient black-silicon solar cell achieved through control of carrier recombination in nanostructures, Nat Nano. 7 (2012) 743-748.

[4] S. Zhong, B. Liu, Y. Xia, J. Liu, J. Liu, Z. Shen, Z. Xu, C. Li, Influence of the texturing structure on the properties of black silicon solar cell, Solar Energy Mater. Solar Cells. 108 (2013) 200-204.

[5] G. Kumaravelu, M.M. Alkaisi, A. Bittar, D. Macdonald, J. Zhao, Damage studies in dry etched textured silicon surfaces, Current Applied Physics. 4 (2004) 108-110.

[6] P. Repo, A. Haarahiltunen, L. Sainiemi, M. Yli-Koski, H. Talvitie, M.C. Schubert, H. Savin, Effective Passivation of Black Silicon Surfaces by Atomic Layer Deposition, Photovoltaics, IEEE Journal of. 3 (2013) 90-94.

[7] T.K. Chong, K.J. Weber, K.M. Booker, A.W. Blakers, Characterization of MAE-Textured Nanoporous Silicon for Solar Cells Application: Optics and Surface Passivation, Photovoltaics, IEEE Journal of. 4 (2014) 1235-1242.

[8] M. Otto, M. Kroll, T. Käsebier, R. Salzer, A. Tünnermann, R.B. Wehrspohn, Extremely low surface recombination velocities in black silicon passivated by atomic layer deposition, Appl. Phys. Lett. 100 (2012) 191603.

[9] H. Savin, P. Repo, G. von Gastrow, P. Ortega, E. Calle, M. Garín, R. Alcubilla, Black silicon solar cells with interdigitated back-contacts achieve 22.1 % efficiency, Nat.Nanotechnol.2015, available online, http://dx.doi.org/10.1038/nnano.2015.89.

[10] G. Agostinelli, A. Delabie, P. Vitanov, Z. Alexieva, H.F.W. Dekkers, S. De Wolf, G. Beaucarne, Very low surface recombination velocities on p-type silicon wafers

passivated with a dielectric with fixed negative charge, Sol. Energ. Mat. Sol. Cells. 90 (2006) 3438-3443.

[11] B. Hoex, J. Schmidt, P. Pohl, M.C.M. van de Sanden, W.M.M. Kessels, Silicon surface passivation by atomic layer deposited Al_2O_3, J. Appl. Phys. 104 (2008) 044903.

[12] G. Dingemans, W.M.M. Kessels, Status and prospects of Al_2O_3-based surface passivation schemes for silicon solar cells, J. of Vac. Sci. & Technol. A: Vac. Surf. Films. 30 (2012) 040802.

[13] B. Hoex, S.B.S. Heil, E. Langereis, M.C.M. van de Sanden, W.M.M. Kessels, Ultralow surface recombination of c-Si substrates passivated by plasma-assisted atomic layer deposited Al_2O_3, Appl. Phys. Lett. 89 (2006) 042112.

[14] A. Mallorquí, E. Alarcón-Lladó, I. Mundet, A. Kiani, B. Demaurex, S. De Wolf, A. Menzel, M. Zacharias, A. Fontcuberta i Morral, Field-effect passivation on silicon nanowire solar cells, Nano Research. 8 (2015) 673-681.

[15] M. Wilson, J. Lagowski, L. Jastrzebski, A. Savtchouk, V. Faifer, COCOS (corona oxide characterization of semiconductor) non-contact metrology for gate dielectrics, AIP Conference Proceedings. 550 (2001) 220-225.

[16] D.K. Schroder, Contactless surface charge semiconductor characterization, Materials Science and Engineering: B. 91–92 (2002) 196-210.

[17] S. Schaefer, R. Lüdemann, Low damage reactive ion etching for photovoltaic applications, Journal of Vacuum Science & Technology A. 17 (1999) 749-754.

[18] S.M. Sze, Physics of Semiconductor Devices, 2nd ed., Wiley, New York, 1981.

[19] B. Hoex, J.J.H. Gielis, M.C.M. van de Sanden, W.M.M. Kessels, On the c-Si surface passivation mechanism by the negative-charge-dielectric Al_2O_3, J. Appl. Phys. 104 (2008) 113703.

[20] B. Kuhlmann, A.G. Aberle, R. Hezel, Two-dimensional numerical optimisation study of inversion layer emitters of silicon solar cells, Proceedings of the 13th European PVSEC, Nice, France. (1995) 1209-1212.

[21] D. Schuldis, A. Richter, J. Benick, P. Saint-Cast, M. Hermle, S.W. Glunz, Properties of the c-Si/Al2O3 interface of ultrathin atomic layer deposited Al2O3 layers capped by SiNx for c-Si surface passivation, Appl. Phys. Lett. 105 (2014).